Natural Resources for Human Health
eISSN: 2583-1194

Original Research

Received 18 Aug 2026
Revised 09 Sep 2026
Accepted 27 Sep 2026

Natural Resources for Human Health 2026, Vol. 6 (23s): 1158–1180

KEYWORDS:
Japanese encephalitis virus; NS2B–NS3 protease; molecular docking; virtual screening; phytochemicals; ADMET; ligand efficiency; andrographolide; kaempferol

In Silico Screening of Natural and Synthetic Compounds Against the NS2B–NS3 Protease of Japanese Encephalitis Virus

Kimaya Jagtap[1], Dr. Amit Jagtap[2]
[1]Dhirubai Ambani International School, Mumbai, 400098
[2]P.D.Hinduja Hospital & Medical Research Center 400052

ABSTRACT: Japanese encephalitis virus (JEV) is an important cause of viral encephalitis, and there is no antiviral treatment available for it at present. Viral NS2B–NS3 serine protease is a crucial component in the processing of the viral polyprotein and is considered a novel target for antiviral drug development. The inhibitory effect of 20 natural and synthetic compounds on JEV NS2B–NS3 protease was evaluated in this study through molecular docking and computational pharmacokinetic and toxicity studies. The crystallographic structure of the protease was used as the receptor to conduct molecular docking using AutoDock4, and the catalytic triad His51, Asp75, and Ser135 were selected as the docking site.

The top compounds were then screened using SwissADME and ProTox 3.0. Ursolic acid showed the lowest docking energy of −6.77 kcal/mol, followed by andrographolide (−6.34 kcal/mol) and kaempferol (−5.80 kcal/mol), in comparison to the reference inhibitor 4-hydroxypanduratin A (−6.31 kcal/mol). Analysis of protein–ligand interactions found interactions with hydrogen-bonding and hydrophobic interactions, in the area surrounding the substrate-binding region. Ursolic acid was predicted to have the best binding affinity; however, due to its high lipophilicity, low gastrointestinal absorption, and potential toxicity, it was not prioritised. Andrographolide and kaempferol showed good drug-likeness, high gastrointestinal absorption potential, and relatively good ligand efficiencies. Kaempferol also exhibited a favourable predicted acute toxicity profile, and andrographolide exhibited binding affinity similar to the reference inhibitor. The synthesized computational results revealed andrographolide and kaempferol as potential molecular scaffolds for further investigations. To prove their therapeutic relevance and to validate their potential as antiviral agents against JEV, experimental enzyme-inhibition assays, cellular antiviral studies, and pharmacokinetic evaluations are necessary.

1. INTRODUCTION

Japanese encephalitis (JE) is a mosquito-borne viral disease and one of the leading causes of epidemic viral encephalitis in Asia. Japanese encephalitis virus (JEV) is a member of the genus Flavivirus, family Flaviviridae, considered to be the major cause of the disease. It is estimated that the number of cases is around 67,900 per year worldwide, but there is a significant under-reporting problem in disease surveillance (Campbell et al., 2011). The disease is more common among children, especially in endemic areas in South and Southeast Asia. In the clinical setting, if infections are severe, they can be associated with seizures, impaired consciousness, neurological effects, and delayed cognitive or behavioural problems. The case fatality rate is around 20-30%, and many survivors have ongoing neurological complications (Solomon, 2003; Turtle et al., 2012).

The main measure of prevention of Japanese encephalitis is vaccination. There are several effective vaccines that have been introduced into national immunisation programmes in endemic countries, which have significantly lowered disease rates in vaccinates. Vaccination alone does not offer therapeutic intervention to people who already have a symptomatic infection. There is no specific antiviral drug available to treat Japanese encephalitis, and management of the clinical condition is largely

supportive, treating seizures and complications (Turtle & Solomon 2018). Therefore, the discovery of novel therapeutic targets of the virus and the development of new antiviral drugs are still significant research goals.

JEV has a positive-sense, single-stranded RNA genome of ~11 kb, with one open reading frame. Translation forms a large polyprotein that is processed into three structural proteins (capsid, precursor membrane/membrane and envelope) and seven non-structural proteins (NS1, NS2A, NS2B, NS3, NS4A, NS4B and NS5) (Chambers, Hahn, et al., 1990). These proteins together control viral entry, genome replication, polyprotein processing, and virion assembly. The non-structural proteins are especially significant as they are involved in the intracellular processes needed for viral replication and propagation.

The NS2B–NS3 protease complex is among these proteins that are good molecular targets for antiviral drug development. NS3 has serine protease activity, and NS2B acts as an essential cofactor to preserve the structural organisation and catalytic activity of the protease in the N-terminal domain. The catalytic machinery consists of three conserved amino acid residues, His51, Asp75 and Ser135, that are involved in the proteolytic reaction. The enzyme catalyzes the polyprotein cleavage of the virus at multiple sites such as NS2A/NS2B, NS2B/NS3, NS3/NS4A and NS4B/NS5. This enzymatic activity is then crucial for the maturation of the viral polyprotein, and thus the essential steps of the replication cycle could be affected (Falgout et al., 1991; Aleshin et al., 2007; Luo et al., 2015).

The structure of the NS2B-NS3 complex gives another rationale to study this protein as a drug target. NS3 has only weak proteolytic activity, but when combined with the hydrophilic cofactor region of NS2B, it has a functional substrate-binding pocket. Structural studies have shown that flaviviral proteases are structurally flexible, with the ability to switch between open and closed conformations. These conformational changes affect both the accessibility of substrates as well as catalytic activity, and may thus offer active-site-directed and potentially allosteric inhibition opportunities (Aleshin et al., 2007; Nitsche, 2019). Moreover, the structural similarity of NS2B–NS3 proteases among flaviviruses implies that inhibitors against conserved structural elements may be relevant to other related viral systems, but this needs to be tested experimentally.

Structure-based studies of the JEV protease have been made possible by the availability of experimentally determined protein structures. Specifically, the crystal structure deposited under PDB accession number 4R8T provides an experimentally determined structure for the study of the interaction between the ligand and the protein and for the identification of regions of the protein that are likely to interact with the inhibitor (Berman et al. 2000). However, finding good inhibitors is difficult as the substrate binding cleft is shallow and solvent-exposed. Such structural features may constrain the development of small molecule inhibitors that have desirable binding affinity, selectivity, and cellular permeability (Nitsche, 2019).

Previous studies have shown that natural products or their derivatives are possible inhibitors of the NS2B–NS3 proteases of flaviviruses. A notable example is 4-hydroxypanduratin A, a cyclohexenyl chalcone that is isolated from Boesenbergia rotunda and is a competitive inhibitor of the NS3 protease of the dengue virus with an inhibition constant of ~21 μM (Kiat et al., 2006). Computational studies of its potential interaction with the JEV protease have also been carried out. These results support the assessment of various naturally occurring compounds with diverse chemical structures on the related flaviviral proteases.

Further experimental research with proteases of dengue and Zika virus has provided direct evidence of the flaviviral proteases' inhibitory potential of flavonoids. De againstusa et al. (2015) showed that some flavonoids such as myricetin and agathisflavone exhibited non-competitive inhibition towards dengue virus NS2B–NS3 proteases. Likewise, Roy et al. (2017) tested the inhibitory activity of natural products against the Zika virus NS2B–NS3 protease and found that myricetin is of particular interest. The presence of antiviral activity has been reported for quercetin, curcumin, luteolin, and related polyphenolic compounds in other investigations. Their inhibitory mechanisms, binding properties, and potencies, however, are different for various viral proteases and experimental conditions.

The secondary metabolites of plants are very rich in antiviral compounds with diverse structures and can be used as a source for preliminary screening of antiviral compounds. Flavonoids, diterpenoids, and stilbenoids have different physicochemical properties and have been shown to have distinct biological activities, such as antiviral activity against various RNA viruses (Zandi et al., 2011; Gupta et al., 2017; Tohmé et al., 2019). Interestingly, compounds like andrographolide and ursolic acid were found to have antiviral effects, while flavonoids like kaempferol and quercetin were studied for their effects on viral proteins.

Nevertheless, the potential of a wider spectrum of natural-product scaffolds targeting the crystallographically resolved JEV NS2B–NS3 protease is still poorly described. Structurally diverse phytochemical screening followed by integrated evaluation of

binding interactions, ligand efficiency, and predicted pharmacokinetic and toxicity properties, for instance, could aid in prioritizing compounds for further experimental investigation.

Computational drug-discovery methods offer an effective initial approach to overcome this gap in research. Molecular docking calculates the orientation and the relative binding affinities of a set of candidate molecules inside a protein binding site, helping to identify possible compounds that have favourable molecular interactions. Docking scores do not, however, provide sufficient data for biological activity. This interpretation should be combined with evaluation of molecular properties, pharmacokinetic properties, and possible toxicity. Lipinski rule of five is the existing guideline for assessing the physicochemical parameters related to oral drug-likeness (Lipinski et al., 2001). SwissADME allows predicting the pharmacokinetic and medicinal chemistry parameters (Daina et al., 2017), and ProTox 3.0 offers the possibility to compute toxicity-related endpoints (Banerjee et al., 2024).

Against this background, the present study employed a structure-based virtual screening approach to investigate the potential of natural and synthetic compounds against the JEV NS2B–NS3 protease. The library of 20 compounds was screened via molecular docking, and 4-hydroxypanduratin A and aspirin were used as positive and negative controls, respectively. The best-performing compounds were then placed under further assessment for their pharmacokinetic and toxicity profiles to develop a comparative evaluation of the compounds' potential for drug development.

The specific objectives were:

- To test the binding potential of 20 natural and synthetic compounds to the crystallographic structure of the NS2B–NS3 protease of JEV.
- To assess molecular interactions and predicted binding affinities of top-ranked compounds in comparison to the reference controls.
- To assess the drug-likeness, predicted pharmacokinetic properties, and toxicity of the shortlist compounds.
- To select candidate molecules to be further subject to experimental investigation based on an integrated assessment of docking performance, ligand efficiency, and predicted developability.

2. MATERIALS AND METHODS

2.1. Hardware and computational software

The computational investigation includes the following steps: protein preparation, ligand preparation, molecular docking, interaction analysis, and in silico pharmacokinetic and toxicity assessment. Protein and ligand preparation, grid generation, and molecular docking were accomplished using AutoDock4 and AutoDockTools 1.5.7. The interaction between the molecules was visualized and analysed using Discovery Studio Visualizer 2025 Client. The drug-likeness and pharmacokinetic properties were assessed through SwissADME (Morris et al., 2009; Daina et al., 2017), and the toxicity predictions were obtained using ProTox 3.0 (Banerjee et al., 2024).

2.2. Protein structure retrieval and preparation

The crystal structure of the NS2B–NS3 protease complex of the Japanese encephalitis virus (JEV) was downloaded from the Research Collaboratory for Structural Bioinformatics Protein Data Bank (RCSB PDB) (Nair et al., 2014). The crystal structure was solved at 2.13 Å resolution by X-ray diffraction, and it shows a protease complex of the Japanese encephalitis virus. The deposited structure consists of the NS2B serine protease cofactor (chain A, 21 amino acid residues) and the NS3 protease domain (chain B, 141 amino acid residues). The deposited protein entities were not reported to contain any mutations.

To prepare the receptor structure for molecular docking, unwanted heteroatoms and unwanted crystallographic constituents were removed. Polar hydrogen atoms were then added, the appropriate charges were assigned, and non-polar hydrogen atoms were bonded to their heavy atom counterparts. The receptor was then converted to PDBQT format using AutoDockTools.

2.3. Identification and definition of the binding site

The catalytic region of the JEV NS2B–NS3 protease was predicted using the known catalytic domain structure of the protease. The His51, Asp75, and Ser135 catalytic triad was selected as the main structural reference to define the docking region.

The selected binding region was centred at the coordinates x = −22.631 Å, y = −28.508 Å, and z = 3.673 Å, with a radius of 7.65 Å. This area was chosen to include the catalytic residues and surrounding amino acids that surround the substrate-binding site.

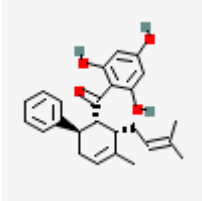
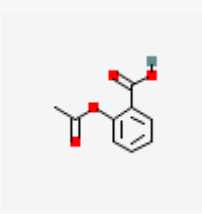
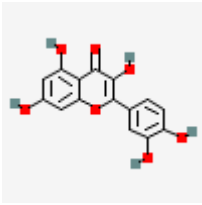
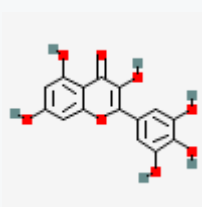
A region of the active site was identified as a reference to create the docking search space and test the predicted binding orientation of the selected compounds.

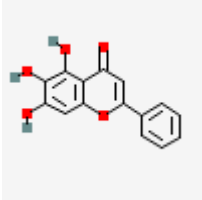
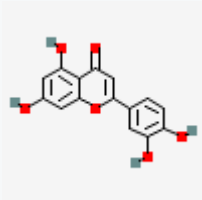
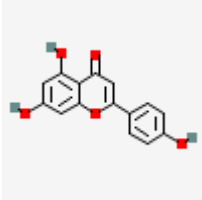
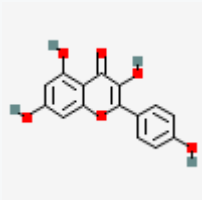
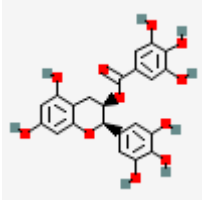
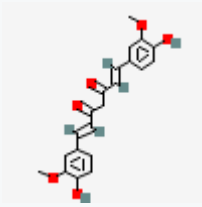
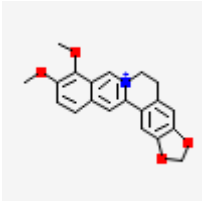
2.4. Ligand library preparation

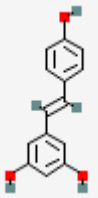
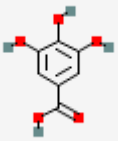
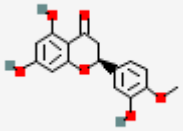
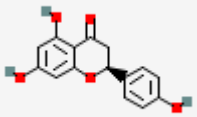
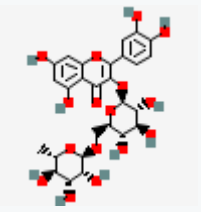
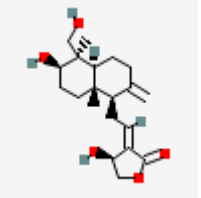
A library of 20 compounds was created, including 16 secondary metabolites from plant sources and four antiviral agents. Flavonoids, flavanones, stilbenoids, alkaloids, phenolic acids, diterpenoids, and triterpenoids were among the natural products present in the natural product library. The antiviral comparators comprised ribavirin, sofosbuvir, favipiravir, and remdesivir.

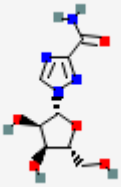
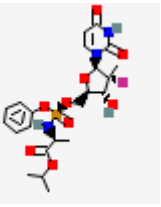
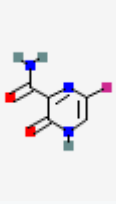
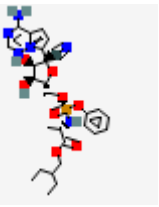
Two-dimensional structures, SMILES notation, and compound identifiers were retrieved from PubChem.

Table 1. 2D Structures, SMILES representations, CID, molecular weight, and molecular formula of controls and test compounds

Control	Compound name	PubChem CID	molecular formula	molecular weight	SMILES	2D Structure
Positive	4-hydroxypanduratin	636530	C25H28O4	392.5 g/mol	CC1=CC[C@H]([C@@H]([C@@H]1CC=C(C)C)C(=O)C2=C(C=C(C=C2O)O)O)C3=CC=CC=C3	
Negative	Aspirin	2244	C9H8O4	180.16 g/mol	CC(=O)OC1=CC=CC=C1C(=O)O	
Test	Quercetin	5280343	C15H10O7	302.23 g/mol	C1=CC(=C(C=C1C2=C(C(=O)C3=C(C=C(C=C3O2)O)O)O)O)O	
	Myricetin	5281672	C15H10O8	318.23 g/mol	C1=C(C=C(C(=C1O)O)O)C2=C(C(=O)C3=C(C=C(C=C3O2)O)O)O	

	Baicalein	5281605	C15H10O5	270.24 g/mol	C1=CC=C(C=C1)C2=CC(=O)C3=C(O2)C=C(C(=C3O)O)O	
	Luteolin	5280445	C15H10O6	286.24 g/mol	C1=CC(=C(C=C1C2=CC(=O)C3=C(C=C(C=C3O2)O)O)O)O	
	Apigenin	5280443	C15H10O5	270.24 g/mol	C1=CC(=CC=C1C2=CC(=O)C3=C(C=C(C=C3O2)O)O)O	
	Kaempferol	5280863	C15H10O6	286.24 g/mol	C1=CC(=CC=C1C2=C(C(=O)C3=C(C=C(C=C3O2)O)O)O)O	
	EGCG	65064	C22H18O11	458.40 g/mol	C1C(C(OC2=CC(=CC(=C21)O)O)C3=CC(=C(C(=C3)O)O)O)OC(=O)C4=CC(=C(C(=C4)O)O)O	
	Curcumin	969516	C21H20O6	368.40 g/mol	COC1=C(C=CC(=C1)C=CC(=O)CC(=O)C=CC2=CC(=C(C=C2)O)OC)O	
	Berberine	2353	C20H18NO4+	336.40 g/mol	COC1=C(C2=C[N+]3=C(C=C2C=C1)C4=CC5=C(C=C4CC3)OCO5)OC	

	Resveratrol	445154	C14H12O3	228.24 g/mol	C1=CC(=CC=C1C=CC2=CC(=CC(=C2)O)O)O	
	Gallic acid	370	C7H6O5	170.12 g/mol	C1=C(C=C(C(=C1O)O)O)C(=O)O	
	Hesperetin	72281	C16H14O6	302.28 g/mol	COC1=C(C=C(C=C1)C2CC(=O)C3=C(C=C(C=C3O2)O)O)O	
	Naringenin	439246	C15H12O5	272.25 g/mol	C1C(OC2=CC(=CC(=C2C1=O)O)O)C3=CC=C(C=C3)O	
	Rutin	5280805	C27H30O16	610.50 g/mol	CC1C(C(C(C(O1)OCC2C(C(C(C(O2)OC3=C(OC4=CC(=CC(=C4C3=O)O)O)C5=CC(=C(C=C5)O)O)O)O)O)O)O)O	
	Andrographolide	5318517	C20H30O5	350.40 g/mol	CC12CCC(C(C1CCC(=C)C2CC=C3C(COC3=O)O)(C)CO)O	
	Ursolic acid	64945	C30H48O3	456.70 g/mol	CC1CCC2(CCC3(C(=CCC4C3(CCC5C4(CCC(C5(C)C)O)C)C)C2C1C)C)C(=O)O	

Antiviral drugs	Ribavirin	37542	C8H12N4O5	244.20 g/mol	C1=NC(=NN1C2C(C(C(O2)CO)O)O)C(=O)N	
	Sofosbuvir	45375808	C22H29FN3O9P	529.50 g/mol	CC(C)OC(=O)C(C)NP(=O)(OCC1C(C(C(O1)N2C=CC(=O)NC2=O)(C)F)O)OC3=CC=CC=C3	
	Favipiravir	492405	C5H4FN3O2	157.10 g/mol	C1=C(N=C(C(=O)N1)C(=O)N)F	
	Remdesivir	121304016	C27H35N6O8P	602.60 g/mol	CCC(CC)COC(=O)C(C)NP(=O)(OCC1C(C(C(O1)(C#N)C2=CC=C3N2N=CN=C3N)O)O)OC4=CC=CC=C4	

The compounds were protonated, and stereochemical assignment and energy minimisation were performed to create three-dimensional structures and prepare them for molecular docking. The ligands were thereafter converted to PDBQT format, and rotatable bonds were defined during the preparation. Based on the chemical structure, Berberine was represented in its quaternary cationic form.

2.5. Selection of reference controls

Based on previous reports of the dengue virus NS3 protease being competitively inhibited by 4-Hydroxypanduratin A, this compound was chosen as a positive control. For comparison, Kiat et al. (2006) reported a literature-based inhibition constant of ~21 μM for this compound based on its structure, which can be useful for the evaluation of the predicted interaction with the JEV protease.

To use Aspirin as a negative control, it was necessary to confirm that it is not known to be an inhibitor of the JEV NS2B–NS3 protease. The binding score predicted by it was used as a comparative reference to evaluate all docked compounds screened.

2.6. Molecular docking

Using AutoDock4, molecular docking was carried out to explore the binding orientation and predicted binding affinities of the selected compounds in the specified binding site of the JEV NS2B–NS3 protease. Receptor and ligand structures were prepared and docked in the PDBQT format, and a grid map was created using AutoGrid.

The Lamarckian genetic algorithm parameters were set as 10 independent docking runs, 150 individuals in each run, 2500000 energy evaluations in each run, and a maximum of 27,000 generations. The two-point crossover mode was used with a crossover rate of 0.80 and a mutation rate of 0.02. This was automatically set to the maximum number of top individuals surviving. The mean and variance of the Cauchy distribution for gene mutation were set to 0.0 and 1.0, respectively, and the number of generations for selecting the worst individual was set to 10.

After docking, the conformation of the generated ligands was analyzed based on their binding energy. The low-energy conformations were chosen for further examination of the protein–ligand interactions. The predicted inhibition constants (Ki) from docking calculations were not experimental values for inhibitory constants (Ki) but were computational estimates (Morris et al., 2009).

2.7. Protein–ligand interaction analysis

The binding conformations of the top-ranked compounds were investigated with BIOVIA Discovery Studio Visualizer. The interactions were classified on the basis of their chemical nature, such as the conventional hydrogen bonds, hydrophobic interactions, aromatic interactions, van der Waals contacts, and unfavourable steric or electrostatic interactions.

Specific interactions between the surrounding residues of the catalytic triad and the nearby substrate-binding cleft were emphasized. All the interacting amino acids and types of interaction were recorded for comparison of shortlisted compounds.

2.8. Prediction of pharmacokinetic properties and drug-likeness

The ten most promising compounds were then evaluated by SwissADME for pharmacokinetic and drug-likeness properties. The parameters evaluated were gastrointestinal absorption, consensus lipophilicity (consensus LogP), Lipinski rule-of-five violations, and predicted bioavailability scores.

The blood–brain barrier permeability was also taken into account, as JEV is a neurotropic virus and it infects the central nervous system. The computational predictions were not considered as evidence of in vivo brain exposure or absorption, but rather as preliminary indicators of compound developability.

2.9. In silico toxicity prediction

ProTox 3.0 was used to determine potential toxicity endpoints. Predicted median lethal dose (LD50), Globally Harmonized System (GHS) toxicity classification, neurotoxicity, hepatotoxicity, immunotoxicity, cardiotoxicity, respiratory toxicity, carcinogenicity and mutagenicity were assessed.

Predicted activity classifications and the associated confidence level were documented. The outcomes were utilised to determine possible safety concerns and to prioritise the compounds for further investigations.

2.10. Integrated selection of candidate compounds

The initial docking results were used to identify the ten highest-ranked compounds for further evaluation. These compounds were then evaluated with respect to their drug-likeness and the pharmacokinetics and toxicity data predicted.

After the comprehensive evaluation of docking affinity, hydrogen bonds, Lipinski violations, gastrointestinal absorption, and gastrointestinal toxicity endpoints, four compounds were shortlisted.

Comparative evaluation of binding affinity, ligand efficiency, predicted pharmacokinetic properties and toxicity concerns resulted in the final choice. Structural diversity was also taken into account for the identification of candidates that were representative of different chemical scaffolds.

3. RESULTS

3.1. Receptor preparation and binding-site characterisation

For molecular docking analysis, the prepared structure of JEV NS2B–NS3 protease (PDB ID: 4R8T) was used. The catalytic triad residues His51, Asp75, and Ser135 were included in the selected active site region. Figure 1 is a representation of the overall structure of the protease and the spatial location of the selected binding region.

Natural Resources for Human Health
eISSN: 2583-1194

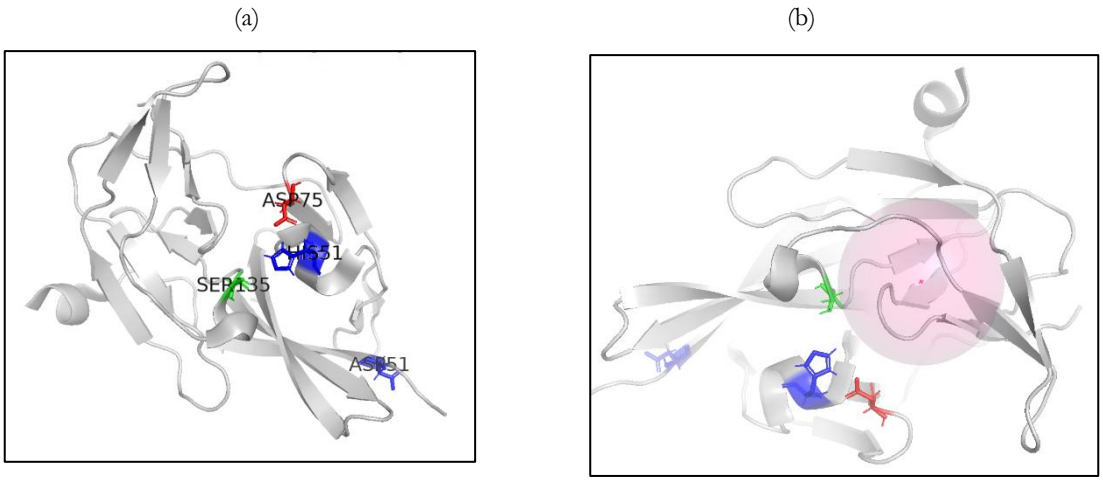


Figure 1. Three-dimensional structure and active-site identification of Japanese encephalitis virus NS2B–NS3 protease. (a) Ribbon representation of the JEV NS2B–NS3 protease complex (PDB ID: 4R8T), highlighting the catalytic triad residues His51, Asp75, and Ser135. (b) Three-dimensional visualization of the protease showing the selected active-site region highlighted as a pink translucent surface, illustrating its spatial location relative to the catalytic residues and surrounding protein structure.

3.2. Molecular docking analysis

The docking assessment revealed appreciable differences in the binding affinities of the screened compounds.

Ursolic acid exhibited the most favourable predicted binding energy of −6.77 kcal/mol, followed by andrographolide (−6.34 kcal/mol), kaempferol (−5.80 kcal/mol), berberine (−5.68 kcal/mol), and quercetin (−5.60 kcal/mol).

T-hydroxypanduratin A was used as a positive control, which showed a docking score of −6.31 kcal/mol with an inhibition constant of 23.51 μM. Aspirin had a significantly lower docking score of −2.91 kcal/mol and a predicted inhibition constant of 7.40 mM.

Table 2. Predicted binding affinities of the highest-ranked compounds and reference controls.

Rank	**Ligand**	**Binding energy (kcal/mol)**	**Predicted Ki**
Positive	4-hydroxypanduratin	−6.31	23.51 μM
Negative	Aspirin	−2.91	7.40 mM
1	Ursolic acid	−6.77	10.94 μM
2	Andrographolide	−6.34	22.41 μM
3	Kaempferol	−5.80	55.78 μM
4	Berberine	−5.68	69.04 μM

5	Quercetin	−5.60	79.15 μM
6	Resveratrol	−5.59	79.70 μM
7	Hesperetin	−5.49	93.97 μM
8	Rutin	−5.45	101.74 μM
9	EGCG	−5.43	105.37 μM
10	Naringenin	−5.41	108.80 μM
11	Baicalein	−5.37	116.58 μM
12	Luteolin	−5.37	116.61 μM
13	Apigenin	−5.34	121.96 μM
14	Myricetin	−5.16	165.12 μM
15	Curcumin	−5.01	210.91 μM
16	Favipiravir	−4.08	1.03 mM
17	Sofosbuvir	-4.05	1.07mM
18	Gallic acid	−3.72	1.88 mM
19	Remdesivir	−3.41	3.17 mM
20	Ribavirin	−2.70	10.49 mM

Ursolic acid and andrographolide among the screened compounds showed predicted binding affinity that is similar to or better than the positive control. Kaempferol, berberine, and quercetin also showed relatively good docking scores; however, they also had lower predicted affinities compared to 4-hydroxypanduratin A.

Ten top compounds were chosen for further pharmacokinetic and toxicology studies.

3.3. Drug-likeness and predicted pharmacokinetic characteristics

A SwissADME analysis showed that there were significant differences between the ten selected compounds in their predicted pharmacokinetic properties.

Andrographolide, kaempferol, berberine, quercetin, resveratrol, hesperetin and naringenin had high predicted gastrointestinal absorption and did not violate any Lipinski rule-of-fives. Although Ursolic acid had the most favourable docking score, it showed 1 violation and a low predicted gastrointestinal absorption.

Both rutin and EGCG had low predicted gastrointestinal absorption. Rutin was found to have 3 violations of the Lipinski rules, while EGCG had 2 violations. Both compounds also had a lower predicted bioavailability score of 0.17.

Table 3. Predicted pharmacokinetic and drug-likeness characteristics of the ten highest-ranked compounds.

Ligand	GI Absorption	Consensus LogP	Lipinski Violations	Bioavailability Score	Drug-Likeness (Lipinski)
Ursolic acid	Low	6.00	1	0.85	Yes
Andrographolide	High	2.43	0	0.55	Yes
Kaempferol	High	1.30	0	0.55	Yes
Berberine	High	2.06	0	0.55	Yes
Quercetin	High	0.95	0	0.55	Yes
Resveratrol	High	2.47	0	0.55	Yes
Hesperetin	High	1.92	0	0.55	Yes
Rutin	Low	−1.75	3	0.17	No
EGCG	Low	0.93	2	0.17	No
Naringenin	High	1.85	0	0.55	Yes

3.4. Predicted toxicity assessment

Ten compounds were selected for the potential toxicity profiles using ProTox 3.0. Ten compounds were selected, and their predicted oral LD50 values were between 159 and 5,000 mg/kg. Rutin had the highest predicted LD50 of 5000 mg/kg, followed by kaempferol at 3919 mg/kg, both of which were allocated to toxicity class 5. Kaempferol had the highest predicted LD50 and the most favorable predicted acute toxicity classification of the four compounds that were shortlisted. Ursolic acid, andrographolide, hesperetin, and naringenin were assigned to toxicity class 4, and berberine and quercetin to toxicity class 3.

Table 4A. Predicted acute toxicity and selected neurological and organ-specific toxicity endpoints

Compound	LD50 (mg/kg)	Class	Neuro	BBB	Hepato	Immuno
Ursolic acid	2000	4	I (0.74)	A (0.69)	A (0.52)	A (0.95)
Andrographolide	1890	4	I (0.94)	A (0.61)	I (0.93)	A (0.82)
Kaempferol	3919	5	I (0.89)	A (0.57)	I (0.68)	I (0.96)
Berberine	200	3	A (0.55)	A (0.85)	I (0.82)	A (0.99)
Quercetin	159	3	I (0.89)	A (0.53)	I (0.69)	I (0.87)
Resveratrol	1560	4	I (0.77)	I (0.55)	I (0.74)	I (0.86)
Hesperetin	2000	4	I (0.87)	I (0.50)	I (0.70)	A (0.90)
Rutin	5000	5	I (0.89)	I (0.75)	I (0.80)	A (0.98)
EGCG	1000	4	I (0.88)	A (0.53)	I (0.70)	I (0.89)
Naringenin	2000	4	I (0.84)	A (0.52)	I (0.67)	I (0.88)

Table 4B. Predicted cardiotoxicity, respiratory toxicity, carcinogenicity and mutagenicity

Compound	Cardio	Respiratory	Carcinogenicity	Mutagenicity
Ursolic acid	A (0.71)	A (0.89)	A (0.57)	I (0.85)
Andrographolide	A (0.55)	A (0.68)	I (0.83)	I (0.71)
Kaempferol	I (0.91)	A (0.83)	I (0.72)	I (0.52)
Berberine	I (0.72)	A (0.76)	A (0.56)	A (0.62)
Quercetin	I (0.99)	A (0.83)	A (0.68)	A (0.51)
Resveratrol	A (0.51)	I (0.57)	I (0.71)	I (0.92)

Hesperetin	A (0.99)	A (0.86)	I (0.70)	I (0.87)
Rutin	I (0.98)	A (0.63)	I (0.91)	I (0.88)
EGCG	I (0.89)	A (0.79)	I (0.54)	I (0.70)
Naringenin	I (0.79)	A (0.82)	I (0.62)	I (0.83)

Note: A = predicted active; I = predicted inactive; values in parentheses indicate the reported prediction confidence. BBB = blood–brain barrier permeability prediction. Neuro = neurotoxicity; Hepato = hepatotoxicity; Immuno = immunotoxicity; Cardio = cardiotoxicity. LD50 = predicted median lethal dose.

3.5. Comparative analysis of protein–ligand interactions

The analysis of protein–ligand interactions of the four shortlisted compounds revealed different patterns of polar, hydrophobic, and aromatic interactions in the selected protease-binding region. Andrographolide and ursolic acid did interact with residues like Glu155 and Val123, while the other residues such as Tyr130, Arg132, Ser127, and Gly151 showed more extensive hydrogen-bond interactions with kaempferol and quercetin. Kaempferol also showed aromatic interactions and less favorable contacts with certain residues. The three-dimensional binding orientations and two-dimensional interaction diagrams are shown in Figures 2–5, and the comparative interaction profiles are summarised in Table 4.

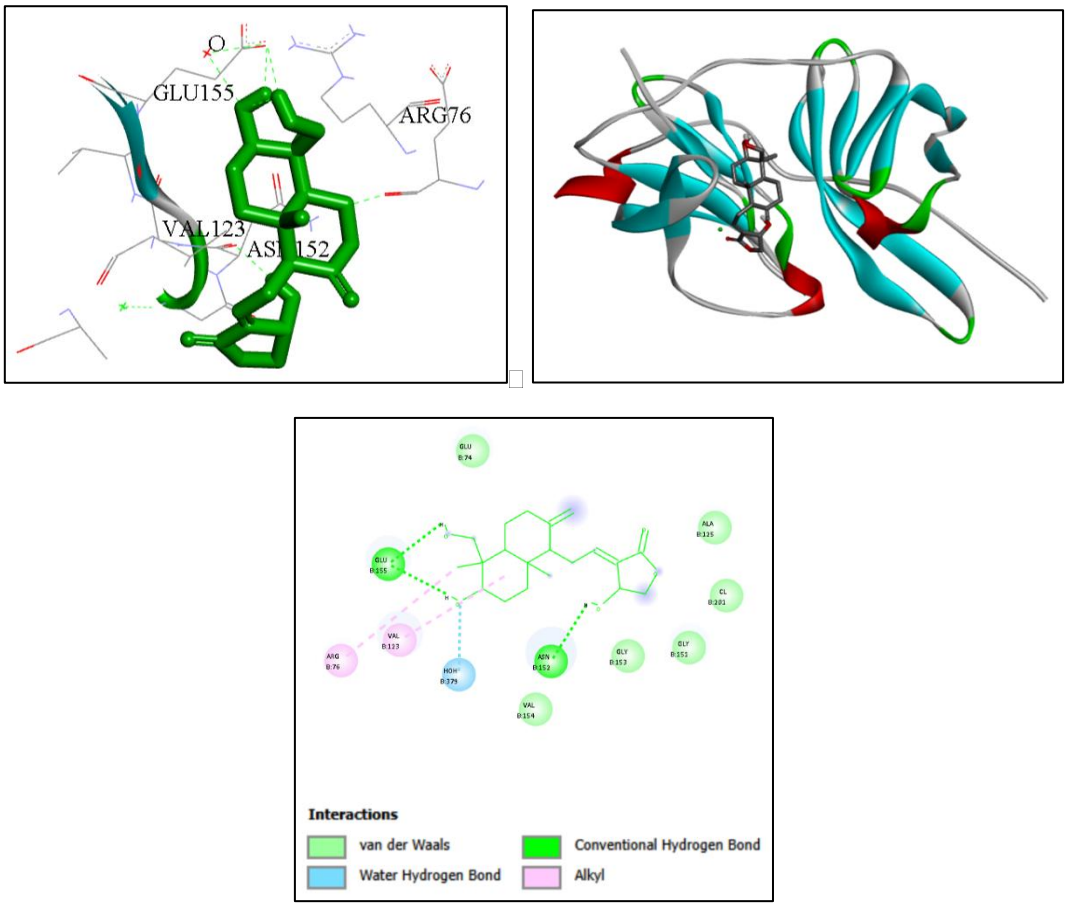


Figure 2. Molecular docking interactions of andrographolide with JEV NS2B–NS3 protease. (a) Three-dimensional representation of the docked andrographolide–protease complex showing the predicted binding orientation of

andrographolide within the selected binding region. (b) Enlarged three-dimensional view illustrating the molecular interactions between andrographolide and neighbouring amino acid residues of the protease. (c) Two-dimensional protein–ligand interaction diagram showing conventional hydrogen bonds with Glu155 and Asn152, hydrophobic interactions involving Val123 and Arg76, and a water-mediated hydrogen bond involving HOH379. Andrographolide exhibited a predicted binding energy of −6.34 kcal/mol.

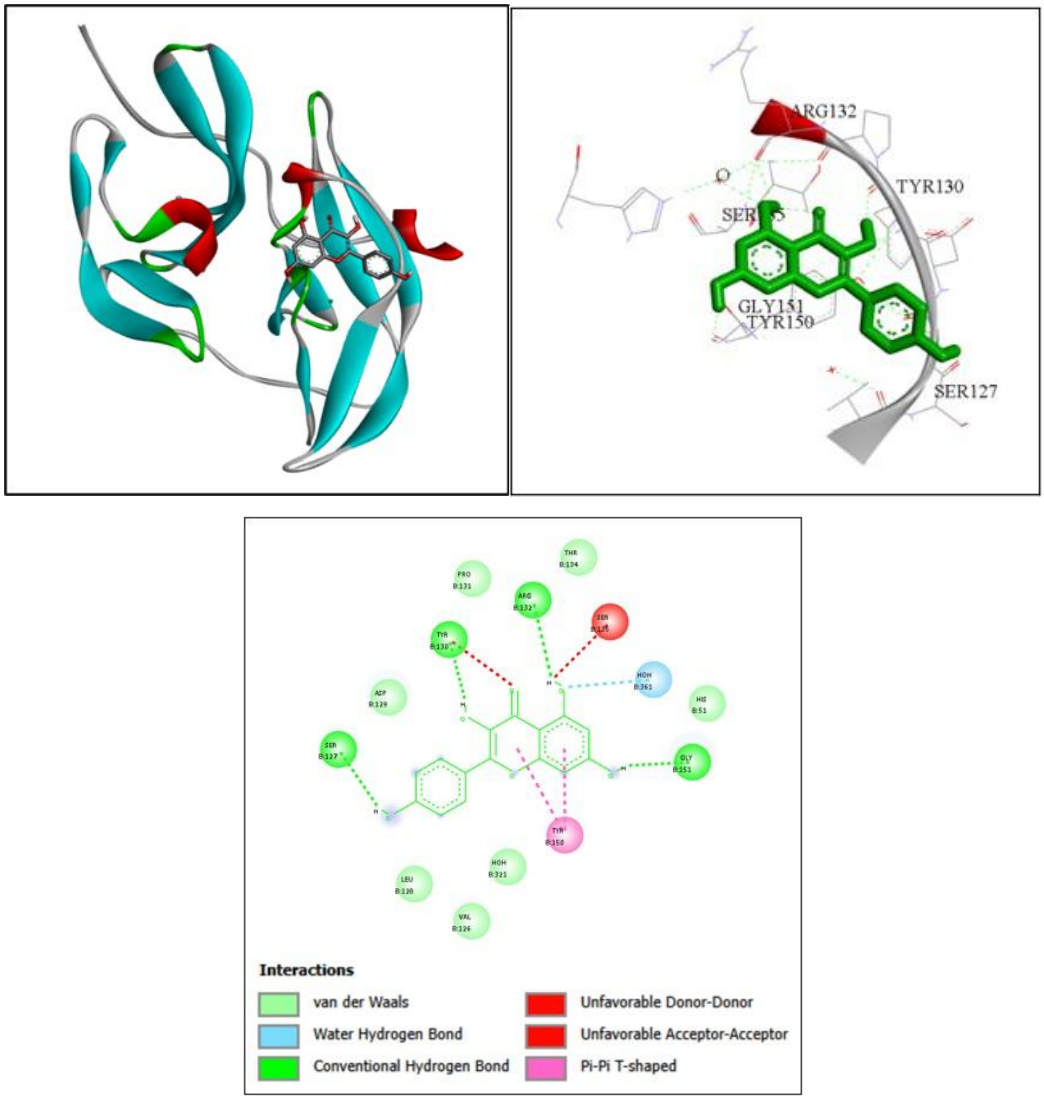


Figure 3. Molecular docking interactions of kaempferol with the JEV NS2B–NS3 protease. (a) Three-dimensional representation of the docked kaempferol–protease complex showing the predicted binding orientation of kaempferol within the selected binding region. (b) Enlarged three-dimensional view highlighting the interactions between kaempferol and surrounding amino acid residues. (c) Two-dimensional protein–ligand interaction diagram illustrating conventional hydrogen bonds with Tyr130, Arg132, Ser127, and Gly151, a π–π T-shaped interaction with Tyr150, and a water-mediated interaction involving HOH361. Unfavourable contacts involving Tyr130 and Ser135 were also identified. Kaempferol exhibited a predicted binding energy of −5.80 kcal/mol.

Natural Resources for Human Health
eISSN: 2583-1194

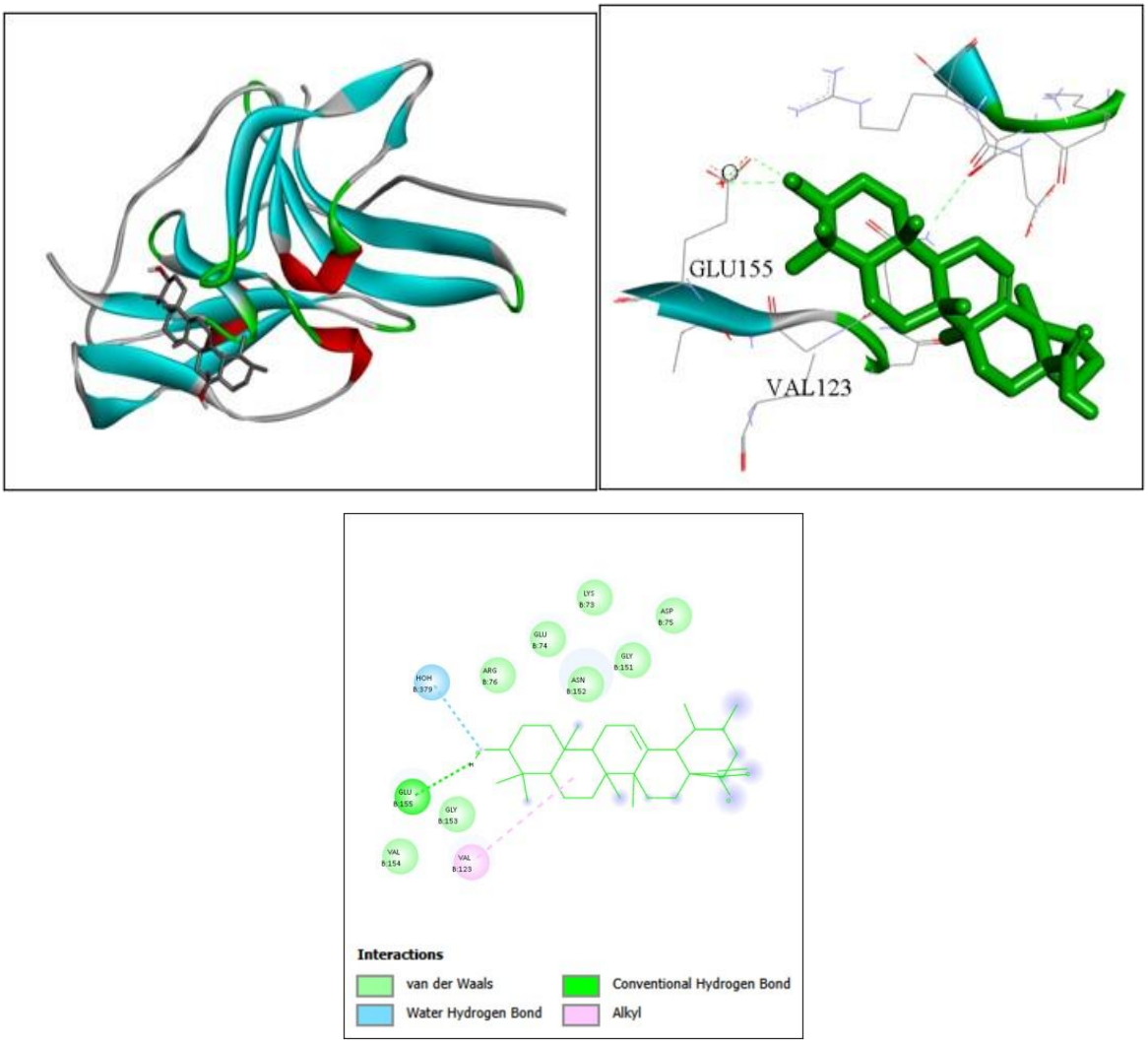


Figure 4. Molecular docking interactions of ursolic acid with JEV NS2B–NS3 protease. (a) Three-dimensional representation of the docked ursolic acid–protease complex illustrating the predicted binding orientation of ursolic acid within the selected binding region. (b) Enlarged three-dimensional view showing the interactions between ursolic acid and neighbouring amino acid residues. (c) Two-dimensional protein–ligand interaction diagram illustrating a conventional hydrogen bond with Glu155, an alkyl interaction involving Val123, and a water-mediated hydrogen bond involving HOH379. Ursolic acid exhibited the most favourable predicted binding energy among the screened compounds (−6.77 kcal/mol).

Natural Resources for Human Health
eISSN: 2583-1194

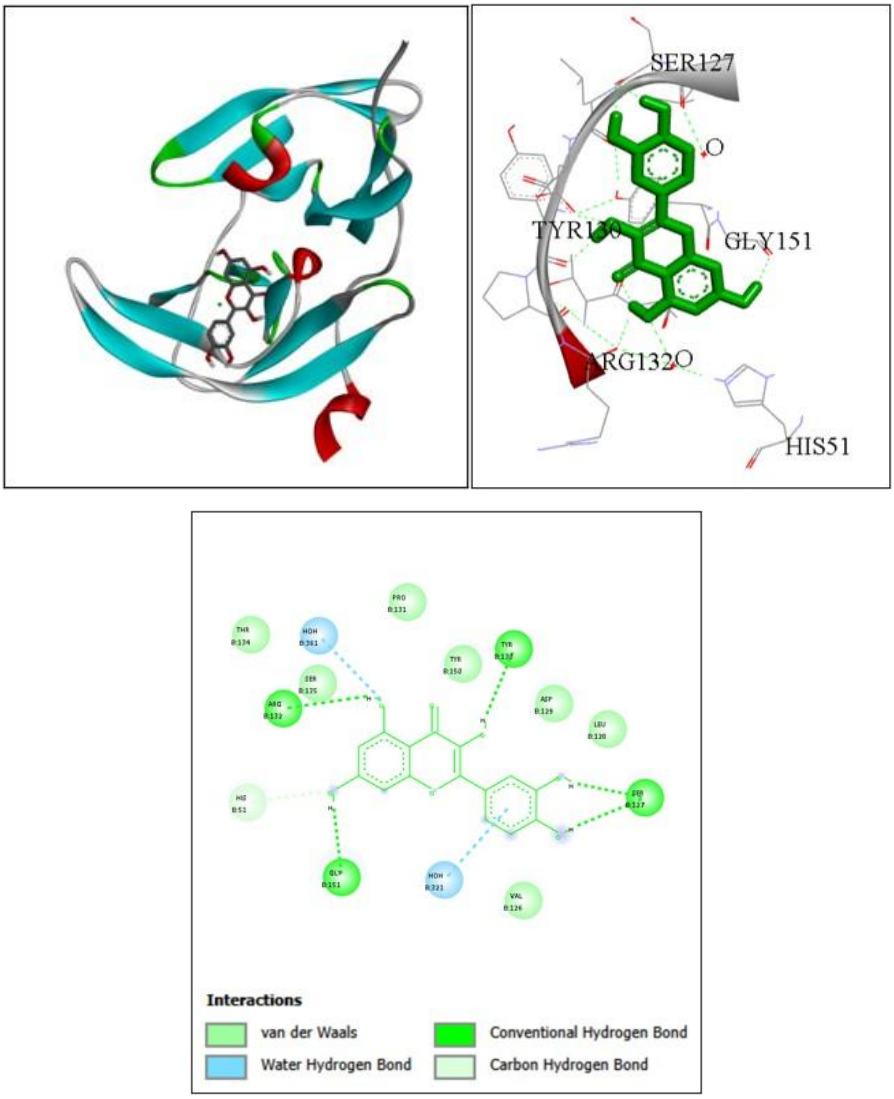


Figure 5. Molecular docking interactions of quercetin with JEV NS2B–NS3 protease. (a) Three-dimensional representation of the docked quercetin–protease complex showing the predicted binding orientation of quercetin within the selected binding region. (b) Enlarged three-dimensional view highlighting the interactions between quercetin and surrounding amino acid residues. (c) Two-dimensional protein–ligand interaction diagram illustrating conventional hydrogen bonds involving Gly151, Arg132, Tyr130, and Ser127, together with a water-mediated hydrogen bond involving HOH361. Quercetin exhibited a predicted binding energy of −5.60 kcal/mol.

Table 5. Comparative interaction profiles of the four shortlisted compounds.

Parameter	**Andrographolide**	**Kaempferol**	**Ursolic acid**	**Quercetin**
Docking energy (kcal/mol)	−6.34	−5.80	−6.77	−5.60
Conventional hydrogen bonds	GLU155, ASN152	TYR130, ARG132, SER127, GLY151	GLU155	TYR130, ARG132, SER127, GLY151

Water-associated contacts observed during visualization	HOH379	HOH361	HOH379	HOH361
Hydrophobic interactions	Alkyl with VAL123 and ARG76	π–π T-shaped with TYR150	Alkyl with VAL123	-
Unfavorable interactions	None shown	TYR130 and SER135 (unfavorable contacts)	None shown	None shown

The interaction profiles showed that the shortlisted compounds bind to the chosen binding site via different sets of polar and nonpolar interactions. For all the reported conventional hydrogen bonds, none involved the catalytic Ser135 residue. Water-associated contacts other than the aforementioned ones were found during the docking ligand conformations visualization process. These water molecules were not considered in the docking calculations, and therefore the observed contacts were not considered as evidence for water-mediated stabilization during docking.

3.6. Comparative ligand-efficiency assessment

The absolute docking score was normalised by the number of heavy atoms in the compound to determine the ligand efficiency. Kaempferol had an average of 0.28 kcal/mol/heavy atom, followed by andrographolide and quercetin with 0.25 and 0.24, respectively. However, for comparison, ursolic acid had a relatively low value of ~0.21 kcal/mol/heavy atom. The positive control had a ligand efficiency around 0.22 kcal/mol/heavy atom.

Table 6. Comparative ligand-efficiency values of selected compounds and reference controls.

Compound	**Heavy atoms**	**Binding energy (kcal/mol)**	**Ligand efficiency (kcal/mol per heavy atom)**
Resveratrol	17	−5.59	0.33
Kaempferol	21	−5.80	0.28
Naringenin	20	−5.41	0.27
Quercetin	22	−5.60	0.25
Andrographolide	25	−6.34	0.25
Hesperetin	22	−5.49	0.25
Berberine	25	−5.68	0.23
Aspirin (negative control)	13	−2.91	0.22

4-Hydroxypanduratin A (positive control)	29	−6.31	0.22
Ursolic acid	33	−6.77	0.21
EGCG	33	−5.43	0.16
Rutin	43	−5.45	0.13

3.7. Prioritisation of final candidate compounds

Two compounds, andrographolide and kaempferol, were chosen for further evaluation based on their integrated binding affinity, ligand efficiency, predicted pharmacokinetic properties and toxicity. Andrographolide had a favourable predicted acute toxicity classification, a comparatively high ligand efficiency, and favourable predicted binding affinity and drug-likeness, whereas kaempferol had a comparatively high ligand efficiency and favourable predicted acute toxicity classification.

Due to its high docking score, it was the most promising; however, because it had high lipophilicity, low predicted gastrointestinal absorption, and potential toxicity liabilities, it was not the most suitable. Quercetin was also not considered due to its less favourable predicted toxicity profile. Therefore, andrographolide and kaempferol were chosen as two different natural-product scaffolds to be further investigated experimentally.

4. DISCUSSION

4.1. Comparative binding characteristics of the screened compounds

The molecular docking results showed that the predicted binding affinity of the compounds screened varied, with ursolic acid and andrographolide being the most promising candidates. However, the small differences in docking energies among the highest-ranked compounds should be interpreted cautiously because scoring functions provide approximate estimates of ligand–protein binding. Aspirin, which has a lower docking ability, served as an additional reference point, but failed to demonstrate docking specificity or inhibition on its own.

These results show that the structurally diverse NPs are good lead compounds for further study. However, docking performance is not enough for the prioritisation of candidates when significant differences exist in molecular dimensions, physico-chemical properties, and predicted toxicity.

The natural products identified with good docking scores are similar to those found in earlier studies, which showed that natural products can bind to flavivirus proteases. De Sousa et al. (2015) found inhibitory activities against dengue virus NS2B–NS3 proteases among selected flavonoids, and Roy et al. (2017) examined the inhibitory potential of natural products against the Zika virus protease. In combination, these studies provide further evidence that structurally diverse natural products are worthy of continued investigation for their potential as starting points for discovery of inhibitors of flaviviral infection.

4.2. Significance of interactions within the protease-binding region

The interaction profiles of the shortlisted compounds indicate that the binding modes of the two molecular scaffolds could be different for the selected protease region. The polar contacts in Andrographolide and the hydrophobic contacts in Kaempferol were found, while Kaempferol made a more extensive hydrogen-bonding network with some unfavourable contacts and aromatic interactions. Although it had the most favourable docking score, Ursolic acid displayed a comparatively limited direct hydrogen-bonding pattern, indicating that it is also influenced by molecular size and non-polar interactions, which could play a role in its predicted binding energy.

Most significantly, no studied compound in the short list of six was able to establish a classical hydrogen bond with the catalytic Ser135 residue. This indication implies that they predict hydrogen-bond interactions within the catalytic region are not direct,

but rather with residues surrounding the catalytic region. A lack of such a hydrogen bond does not rule out other interactions with the catalytic machinery, nor does it rule out a specific mechanism of inhibition.

It has been previously shown that flaviviral NS2B–NS3 proteases are conformationally flexible and can adopt open or closed conformations (Aleshin et al., 2007). Some of the flavonoids have also been known to show non-competitive inhibition of dengue and Zika proteases (de Sousa et al., 2015; Roy et al., 2017). The findings give a mechanistic background for the investigations of peripheral binding reactions. However, the present docking results do not suggest whether the action of andrographolide or kaempferol is competitive, non-competitive, or allosteric.

4.3. Comparison with previously investigated flaviviral protease inhibitors

As a positive control, 4-Hydroxypanduratin A was used as it is known to inhibit the dengue virus NS3 protease. Kiat et al. (2006) reported an experimental inhibition constant of ~21 μM for this compound.

In the present study, 4-hydroxypanduratin A was found to have a predicted docking energy of −6.31 kcal/mol and a predicted inhibition constant of 23.51 μM. The docking protocol is not directly validated by the comparison of the predicted value with the reported experimental inhibition constant, as the proteases used are taken from different flaviviruses.

All the shortlisted compounds had predicted inhibition constants within the micromolar range. The predicted value of andrographolide was 22.41 μM, kaempferol had a predicted value of 55.78 μM, and ursolic acid had a predicted value of 10.94 μM.

Previous studies of flavonoids for inhibition of the dengue virus proteases have shown their inhibitory properties to be in the micromolar range. Several flavonoids have been reported in a study by De Sousa et al. (2015) having inhibitory activity against dengue NS2B–NS3 proteases and particularly myricetin against Zika protease by Roy et al. (2017).

The present predictions have been provided with a biochemical comparison. Due to differences in the structure of the viral protease, the conditions of the assay, protein conformational states, and experimental methods, however, the docking-derived inhibition constants cannot be directly compared with the experimentally derived IC50 or Ki values.

4.4. Pharmacokinetic properties and drug-likeness

The pharmacokinetic evaluation revealed the need to consider the physicochemical properties in addition to the predicted binding. Ursolic acid showed the best docking score, but was also highly lipophilic with a low predicted gastrointestinal absorption, which is a possible hurdle in oral drug development. However, andrographolide and kaempferol had more favorable predicted absorption and drug-likeness properties.

The unfavorable profiles of rutin and EGCG further highlight that the molecular features associated with molecular recognition do not necessarily equate to desirable PK properties. To conclude, these results lend support to the idea of screening the candidates not only by docking scores, but also by using integrated computational screening (Lipinski et al., 2001; Daina et al., 2017). However, the foretold parameters should be experimentally substantiated.

4.5. Comparative toxicity profiles of the shortlisted compounds

The predicted toxicity profiles provided an additional criterion to differentiate the shortlisted compounds. While not all four candidates were found to have a favourable predicted acute toxicity classification, kaempferol emerged as the most favorable candidate, with the exception of its respiratory toxicity prediction. However, andrographolide showed a less desirable profile in some organ-specific toxicity endpoints, suggesting its positive docking properties need to be weighed against the potential toxicity issues.

Ursolic acid and quercetin had other predicted toxicity issues that did not make them suitable for prioritisation, even though they demonstrated favourable molecular interactions. The results show that the overall therapeutic potential of a compound is not necessarily reflected by the predicted binding affinity. Most importantly, the prediction results from ProTox 3.0 are only estimates, and should not be regarded as experimentally determined toxicity or safety data.

4.6. Ligand efficiency and prioritisation of final candidates

The differences in molecular size were taken into account by using Ligand efficiency as a perspective of the docking result. Ligand efficiency is comparatively low for ursolic acid, and thus its favourable docking energy could be attributed partially to its larger molecular structure. In comparison, kaempferol showed relatively efficient predicted binding per heavy atom, which helps it to be considered a smaller scaffold for further optimisation.

Andrographolide had the complementary profile, being favorable for the predicted binding affinity and good drug-likeness characteristics for the screening criteria adopted. Selection of Andrographolide (labdane diterpenoid) and Kaempferol (flavonol) also offers structural diversity for further studies. They have unique chemical structures that could provide a range of different opportunities to optimise binding interactions and physicochemical properties.

However, the docking-derived ligand efficiency should be viewed as a computational, comparative measure of binding efficiency and not as a true experimental measure of binding efficiency.

4.7. Relevance to central nervous system exposure

The neurotropic nature of JEV adds another important factor for designing potential anti-JEV compounds – their ability to reach therapeutic levels in the central nervous system. Both andrographolide and kaempferol were predicted to have the potential to cross the blood–brain barrier by SwissADME and ProTox 3.0. These forecasts give a preliminary sense of their potential suitability in the context of Japanese encephalitis for further investigation.

However, the predicted blood–brain barrier permeability does not provide sufficient central nervous system exposure. Brain distribution can be significantly impacted by compound-specific factors such as plasma protein binding, metabolic stability, transporter-mediated efflux, and the formation of active or inactive metabolites. Therefore, it is crucial to conduct experiments for the measurement of plasma and brain levels of these compounds prior to the consideration of either as potential candidates for the treatment of a neurotropic viral infection.

4.8. Study limitations and future research directions

In the present study, we present a preliminary computational evaluation for natural and synthetic compounds targeting the JEV NS2B–NS3 protease. The results need to be interpreted with caution, however, because of some methodological constraints.

Molecular docking provides an approximate prediction of the interactions between the ligand and the protein, but does not directly show the inhibitory activity. Moreover, the flexibility of the receptor and the use of a single crystallographic receptor conformation might not be sufficient to cover the dynamic behaviour of the protease and/or ligand-induced conformational changes. The effects of solvent and the entropic contributions on the binding affinity and relative ranking of compounds might also be affected by the simplified treatment.

A drawback is the lack of independent validation of the docking procedure with an experimentally validated inhibitor–protease complex. The chosen crystal structure (PDB ID: 4R8T) does not contain an organic inhibitor co-crystallised with the crystal structure to be used for conventional redocking validation. 4-Hydroxypanduratin A was chosen as a positive literature control compound, but the reported inhibitory activity was towards dengue virus protease and not towards JEV NS2B–NS3 protease. Thus, these calculated binding energies and inhibition constants should be considered as preliminary computational values, and not as measured values of inhibitory potency.

In addition, the pharmacokinetic and toxicity properties are computed and remain to be experimentally validated, especially in the central nervous system and organ-specific toxicity. There is a lack of biochemical and cell-based validation, which further restricts conclusions on the antiviral efficacy of the prioritised compounds.

Future studies should include biochemical assays using JEV NS2B–NS3 protease to assess the inhibitory activity of future testing of andrographolide and kaempferol and determine experimental IC50 and Ki values, as well as the mechanism of inhibition. Antiviral and cytotoxicity assays at the cellular level would further confirm their antiviral activity and selectivity. Molecular dynamics simulations could further assess the stability and conformational behaviour of the predicted protein–ligand complexes, while experimental pharmacokinetic and central nervous system exposure studies would provide additional evidence to support their potential for further drug development.

5. CONCLUSION

In this study, two potential natural-product scaffolds, namely andrographolide and kaempferol, were identified using integrated molecular docking, ligand-efficiency, pharmacokinetic, and toxicity evaluations against the JEV NS2B–NS3 protease. The overall computational profiles, while ursolic acid had the best predicted binding energy, indicated prioritisation for andrographolide and kaempferol. They have different chemical structures and complementary predicted properties, giving a reason for further research. However, activity in biochemical enzyme-inhibition assays, cell-based antiviral studies, and experimental pharmacokinetic and toxicity evaluations are crucial to determine their inhibitory activity, safety, and therapeutic relevance against JEV.

ACKNOWLEDGEMENTS

I would like to thank my teachers, parents, and friends for their guidance and support.

AUTHOR CONTRIBUTIONS

Dr Amit Jagtap: Conceptualisation, Investigation.

Kimaya Jagtap: Literature review and data analysis

Kimaya Jagtap: Manuscript Drafting

Dr Amit Jagtap: Supervision, Writing—Review & Editing.

CONFLICT OF INTEREST

The author declares no conflicts of interest to disclose.

ETHICS STATEMENT

This manuscript is a literature-based review of previously published research and does not involve the recruitment of human participants, collection of primary patient data, or experimentation on animals. Therefore, institutional ethics committee approval and informed consent were not required for the preparation of this review.

DATA AVAILABILITY STATEMENT

Data supporting the findings of this study are available from the corresponding author upon reasonable request.

REFERENCES

[1] Aleshin, A. E., Shiryaev, S. A., Strongin, A. Y., & Liddington, R. C. (2007). Structural evidence for regulation and specificity of flaviviral proteases and evolution of the flaviviridae fold. *Protein Science*, *16*(5), 795–806. https://doi.org/10.1110/ps.072753207

[2] Apex Bioinformatics Centre, Department of Biotechnology, Ministry of Science and Technology, Lodhi Road, New Delhi – 110 003, India, Seniya, C., Mishra, H., Yadav, A., Sagar, N., Chaturvedi, B., Uchadia, K., & Wadhwa, G. (2013). Antiviral potential of 4-hydroxypanduratin A, a secondary metabolite of fingerroot, Boesenbergia Pandurata (Schult.) against Japanese encephalitis virus NS2B/NS3 protease. *Bioinformation*, *9*(1), 54–60. https://doi.org/10.6026/97320630009054

[3] Banerjee, P., Kemmler, E., Dunkel, M., & Preissner, R. (2024). ProTox 3.0: A web server for the prediction of toxicity of chemicals. *Nucleic Acids Research*, *52*(W1). https://doi.org/10.1093/nar/gkae303

[4] Berman, H. M., Battistuz, T., Bhat, T. N., Bluhm, W. F., Bourne, P. E., Burkhardt, K., Feng, Z., Gilliland, G. L., Iype, L., Jain, S., Fagan, P., Marvin, J., Padilla, D., Ravichandran, V., Schneider, B., Thanki, N., Weissig, H., Westbrook, J. D., & Zardecki, C. (2002). The Protein Data Bank. *Acta Crystallographica Section D: Biological Crystallography*, *58*(6), 899–907. https://doi.org/10.1107/s0907444902003451

[5] Campbell, G., Hills, S., Fischer, M., Jacobson, J., Hoke, C., Hombach, J., Marfin, A., Solomon, T., Tsai, T., Tsui, V., & Ginsburg, A. (2011). Estimated global incidence of Japanese encephalitis: *Bulletin of the World Health Organization*, *89*(10), 766–774. https://doi.org/10.2471/blt.10.085233

[6] Chambers, T. J., Hahn, C. S., Galler, R., & Rice, C. M. (1990). Flavivirus genome organization, expression, and replication. *Annual Review of Microbiology*, *44*(1), 649–688. https://doi.org/10.1146/annurev.mi.44.100190.003245

[7] Chambers, T. J., Weir, R. C., Grakoui, A., McCourt, D. W., Bazan, J. F., Fletterick, R. J., & Rice, C. M. (1990). Evidence that the N-terminal domain of nonstructural protein NS3 from yellow fever virus is a serine protease responsible for site-specific cleavages in the viral polyprotein. *Proceedings of the National Academy of Sciences*, *87*(22), 8898–8902. https://doi.org/10.1073/pnas.87.22.8898

[8] Daina, A., Michielin, O., & Zoete, V. (2017). SwissADME: A free web tool to evaluate pharmacokinetics, drug-likeness and medicinal chemistry friendliness of small molecules. *Scientific Reports*, *7*(1), 1–13. https://doi.org/10.1038/srep42717

[9] de Sousa, L. R. F., Wu, H., Nebo, L., Fernandes, J. B., da Silva, M. F. das G. F., Kiefer, W., Kanitz, M., Bodem, J., Diederich, W. E., Schirmeister, T., & Vieira, P. C. (2015). Flavonoids as noncompetitive inhibitors of dengue virus NS2B-NS3 protease: Inhibition kinetics and docking studies. *Bioorganic & Medicinal Chemistry*, *23*(3), 466–470. https://doi.org/10.1016/j.bmc.2014.12.015

[10] Falgout, B., Pethel, M., Zhang, Y. M., & Lai, C. J. (1991). Both nonstructural proteins NS2B and NS3 are required for the proteolytic processing of dengue virus nonstructural proteins. *Journal of Virology*, *65*(5), 2467–2475. https://doi.org/10.1128/jvi.65.5.2467-2475.1991

[11] Gupta, S., Mishra, K. P., & Ganju, L. (2016). Broad-spectrum antiviral properties of andrographolide. *Archives of Virology*, *162*(3), 611–623. https://doi.org/10.1007/s00705-016-3166-3

[12] Kiat, T. S., Pippen, R., Yusof, R., Ibrahim, H., Khalid, N., & Rahman, N. A. (2006). Inhibitory activity of cyclohexenyl chalcone derivatives and flavonoids of fingerroot, Boesenbergia rotunda (L.), towards dengue-2 virus NS3 protease. *Bioorganic & Medicinal Chemistry Letters*, *16*(12), 3337–3340. https://doi.org/10.1016/j.bmcl.2005.12.075

[13] Kim, S., Chen, J., Cheng, T., Gindulyte, A., He, J., He, S., Li, Q., Shoemaker, B. A., Thiessen, P. A., Yu, B., Zaslavsky, L., Zhang, J., & Bolton, E. E. (2022). PubChem 2023 update. *Nucleic Acids Research*, *51*(D1). https://doi.org/10.1093/nar/gkac956

[14] Lipinski, C. A., Lombardo, F., Dominy, B. W., & Feeney, P. J. (2001). Experimental and computational approaches to estimate solubility and permeability in drug discovery and development settings. *Advanced Drug Delivery Reviews*, *46*(1–3), 3–26. PubMed. https://doi.org/10.1016/s0169-409x(00)00129-0

[15] Luo, D., Vasudevan, S. G., & Lescar, J. (2015). The flavivirus ns2b–NS3 protease–helicase as a target for antiviral drug development. *Antiviral Research*, *118*, 148–158. https://doi.org/10.1016/j.antiviral.2015.03.014

[16] Morris, G. M., Huey, R., Lindstrom, W., Sanner, M. F., Belew, R. K., Goodsell, D. S., & Olson, A. J. (2009). AutoDock4 and AutoDockTools4: Automated docking with selective receptor flexibility. *Journal of Computational Chemistry*, *30*(16), 2785–2791. PubMed. https://doi.org/10.1002/jcc.21256

[17] Nair, D. T., Weinert, T., Wang, M., & Olieric, V. (2014). *Structure of JEV protease*. https://doi.org/10.2210/pdb4r8t/pdb

[18] Nitsche, C. (2019). Proteases from Dengue, West Nile and Zika viruses as drug targets. *Biophysical Reviews*, *11*(2), 157–165. https://doi.org/10.1007/s12551-019-00508-3

[19] Noble, C. G., Chen, Y.-L., Dong, H., Gu, F., Lim, S. P., Schul, W., Wang, Q.-Y., & Shi, P.-Y. (2010). Strategies for development of dengue virus inhibitors. *Antiviral Research*, *85*(3), 450–462. https://doi.org/10.1016/j.antiviral.2009.12.011

[20] Quan, T. M., Thao, T. T. N., Duy, N. M., Nhat, T. M., & Clapham, H. (2020). Estimates of the global burden of Japanese encephalitis and the impact of vaccination from 2000-2015. *eLife*, *9*, e51027. https://doi.org/10.7554/eLife.51027

[21] Roy, A., Lim, L., Srivastava, S., Lu, Y., & Song, J. (2017). Solution conformations of Zika NS2B-NS3pro and its inhibition by natural products from edible plants. *PLOS ONE*, *12*(7), e0180632. https://doi.org/10.1371/journal.pone.0180632

[22] Solomon, T. (2003). Recent advances in Japanese encephalitis. *Journal of Neurovirology*, *9*(2), 274–283. https://doi.org/10.1080/13550280390194037

[23] Tohmé, M. J., Giménez, M. C., Peralta, A., Colombo, M. I., & Delgui, L. R. (2019). Ursolic acid: A novel antiviral compound inhibiting rotavirus infection in vitro. *International Journal of Antimicrobial Agents*, *54*(5), 601–609. https://doi.org/10.1016/j.ijantimicag.2019.07.015

[24] Turtle, L., Griffiths, M. J., & Solomon, T. (2012). Encephalitis caused by flaviviruses. *QJM*, *105*(3), 219–223. https://doi.org/10.1093/qjmed/hcs013

[25] Turtle, L., & Solomon, T. (2018). Japanese encephalitis — The prospects for new treatments. *Nature Reviews Neurology*, *14*(5), 298–313. https://doi.org/10.1038/nrneurol.2018.30

[26] Wang, X., Li, S.-H., Zhu, L., Nian, Q.-G., Yuan, S., Gao, Q., Hu, Z., Ye, Q., Li, X.-F., Xie, D.-Y., Shaw, N., Wang, J., Walter, T. S., Huiskonen, J. T., Fry, E. E., Qin, C.-F., Stuart, D. I., & Rao, Z. (2017). Near-atomic structure of Japanese

encephalitis virus reveals critical determinants of virulence and stability. *Nature Communications*, *8*(1), 14. PubMed. https://doi.org/10.1038/s41467-017-00024-6

[27] Zandi, K., Teoh, B.-T., Sam, S.-S., Wong, P.-F., Mustafa, M. R., & AbuBakar, S. (2011). Antiviral activity of four types of bioflavonoids against dengue virus type 2. *Virology Journal*, *8*(1), Article 560. https://doi.org/10.1186/1743-422x-8-560